

Provably-Safe Neural Network Training Using Hybrid Zonotope Reachability Analysis

Long Kiu Chung and Shreyas Kousik

Abstract—Even though neural networks are being increasingly deployed in safety-critical applications, it remains difficult to enforce constraints on their output, meaning that it is hard to guarantee safety in such settings. Towards addressing this, many existing methods seek to *verify* a neural network’s satisfaction of safety constraints, but do not address how to correct an “unsafe” network. On the other hand, the few works that extract a training signal from verification cannot handle non-convex sets, and are either conservative or slow. To address these challenges, this work proposes a neural network training method that can encourage the *exact* reachable set of a non-convex input set through a neural network with rectified linear unit (ReLU) nonlinearities to avoid a non-convex unsafe region, using recent results in non-convex set representation with hybrid zonotopes and extracting gradient information from mixed-integer linear programs (MILPs). The proposed method is fast, with the computational complexity of each training iteration comparable to that of solving a linear program (LP) with number of dimensions and constraints *linear* to the number of neurons and complexity of input and unsafe sets. For a neural network with three hidden layers of width 30, the method was able to drive the reachable set of a non-convex input set with 55 generators and 26 constraints out of a non-convex unsafe region with 21 generators and 11 constraints in 490 seconds.

I. INTRODUCTION

Neural networks are universal approximators [1] that have seen success in many domains. However, they are also well-known as “black-box” models, where the relationship between their inputs and outputs is not easily interpretable or directly analyzable due to non-linearity and high-dimensional parameterizations. As such, it is very difficult to certify their *safety* (e.g. satisfaction of constraints). This limitation imposes many significant drawbacks. For example, robots crash frequently when training their neural network controllers with deep reinforcement learning (RL) algorithms, limiting deep RL’s success in robots where hardware failures are costly, simulations are not readily available, or the sim-to-real gap is too large for reliable performance [2]. In addition, neural networks can also be susceptible to adversarial attacks, where minor perturbations in the input can lead to drastically different results in the output [3], [4]. This makes deploying neural networks in *safety-critical* tasks a questionable choice, even though it has already been widely done [5]–[7], leading to many injuries and accidents [8]. In this paper, we present a method to enforce safety in neural networks by encouraging their satisfaction of a collision-free constraint, which has potential application in making deep RL safe, neural networks

robust to adversarial attacks, and more. An overview of our method is shown in Fig. 1.

A. Related Work

We now review three key approaches to enforce constraints on neural network: sampling-based approaches that do not have formal guarantees, verification approaches that only check constraint satisfaction, and approaches that combine verification with training, which our method belongs to. Finally, we review relevant literature on *hybrid zonotopes*, which is the set representation used in our method.

1) *Training with Soft Constraints*: Many existing work capture safety in neural networks by penalizing constraint violations on sampled *points* during training [9]–[13]. However, these *soft* approaches, while often fast and easy to implement, do not provide any safety guarantees beyond the training samples. While there are works that are capable of enforcing *hard* constraints in neural networks by modifying the training process [14], [15], they can only handle simple affine constraints.

2) *Neural Network Verification*: A different approach is to certify safety with respect to a *set* of inputs. Methods in this category tend to analyze the *reachable set* (i.e. image) of the input set through the neural network, either exactly [16]–[20] or as an over-approximation [16]–[18], [21]–[23] depending on the choice of set representation. That said, most of these works only focus on neural network *verification*. That is, these methods only answer the yes-no question of “safe” or “unsafe”, with the aftermath of fixing an “unsafe” network left largely unexplored. As a result, engineers can only train via trial-and-error until the desired safety properties have been achieved, which can be slow and ineffective.

3) *Training with Verification*: To the best of our knowledge, there are only two works that attempted to extract *learning signals* from the safety verification results using reachability analysis.

First, in [24], given an input set as an H-polytope (i.e. polytope represented by intersection of halfplanes) and a neural network controller embedded in a nonlinear dynamical system, the polytope is expressed as the projection of a high-dimensional hyperrectangle, enabling the use of the CROWN verifier [21] for interval reachability. Then, using a loss function that encourages the vector field of the reachable set to point inwards, the authors were able to train the neural network until the system is *forward invariant*. With this method, the input set is limited to being a convex polytope. Moreover, since [21] and the interval reachability techniques used are

All authors are with the Department of Mechanical Engineering, Georgia Institute of Technology, Atlanta, GA. Corresponding author: shreyas.kousik@me.gatech.edu.

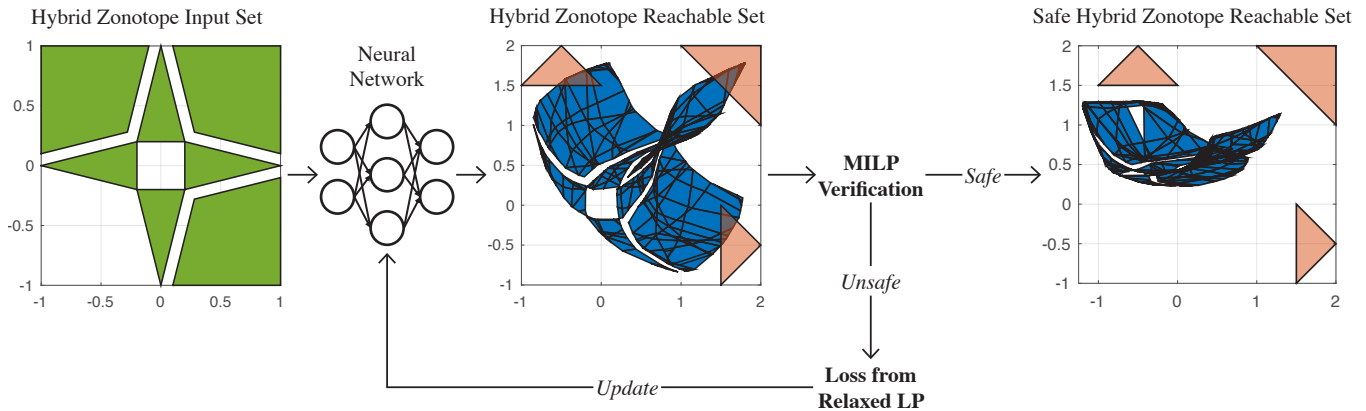


Fig. 1. A flowchart of our method, using the example from Sec. VI. Our method takes in a non-convex input set (green), then computes its *exact* reachable set (blue) through the neural network. Then, we formulate the reachable set’s collision with the unsafe set (red) as a loss function using a linear program (LP), which enables us to update the neural network’s parameters via backpropagation. Every several iterations, we check if the reachable set collides with the unsafe set using a mixed-integer linear program (MILP). If it does not, then the training is complete and our method is successful.

over-approximations, its space of discoverable solutions may be limited.

Second, given an input set and an unsafe region expressed as constrained zonotopes (a convex polytopic representation [25]), our prior work [26] computed the *exact* reachable set of a neural network as a union of constrained zonotopes. Then, by using a loss function to quantify the “emptiness” of the intersection between the reachable set and the unsafe region, we were able to train the neural network such that the reachable set no longer collides with the unsafe region. Similarly, the input set and the obstacle in this method is limited to being a convex polytope. Moreover, the number of sets needed to represent the reachable set grows exponentially with the size of the neural network, making the method numerically intractable even for very small neural networks.

4) *Hybrid Zonotopes*: Recently, a non-convex polytopic set representation called the hybrid zonotope [27] was proposed. Hybrid zonotopes are closed under affine mapping, Minkowski sum, generalized intersection, intersection [27], union, and complement [28], with extensive toolbox support in MATLAB [29] and Python [30]. They can also exactly represent the *forward reachable set* (image) [19] and *backward reachable set* (preimage) [31] of a neural network with rectified linear units (ReLU) using basic matrix operations, with complexity scaling only linearly with the size of the network. However, existing methods for hybrid zonotopes enforce safety on robots either by formulating a model predictive control (MPC) [28] or a nonlinear optimization problem [32] without neural networks in the loop, whereas those with neural networks only use hybrid zonotope for verification but not training [19], [31], [33], [34]. In this paper, our contribution is extracting and using learning signals from neural network reachability analysis with hybrid zonotopes.

B. Contributions

Our contributions are twofold:

- 1) Given a non-convex input set and a non-convex unsafe region, we propose a differentiable loss function for

ReLU neural networks training based on *exact* reachability analysis with hybrid zonotope. This loss function encourages the reachable set of the input set to avoid the unsafe region, the satisfaction of which can be checked using a mixed-integer linear program (MILP).

- 2) We show that this method is fast and scales fairly well with respect to input dimensions, output dimensions, network size, complexity of the input set, and complexity of the unsafe region. The results significantly outperform our prior method for exact reachability analysis in training [26].

The remainder of the paper is organized as follows: we provide preliminary information in Sec. II, formalize our problem statement in Sec. III, detail our proposed method in Sec. IV, provide experimental analysis in Sec. V, demonstrate the utility of our method in Sec. VI, then give concluding remarks and limitations in Sec. VII.

II. PRELIMINARIES

We now introduce our notation conventions, define hybrid zonotopes and ReLU neural networks, and summarize existing work [19], [31] on representing image of a hybrid zonotope through a ReLU neural network exactly as a hybrid zonotope.

A. Notation

In this paper, we denote the set of real numbers as \mathbb{R} , non-negative real numbers as \mathbb{R}_+ , natural numbers as \mathbb{N} , scalars in lowercase italic, sets in uppercase italic, vectors in lowercase bold, and matrices in uppercase bold. We also denote a matrix of zeros as $\mathbf{0}$, a matrix of ones as $\mathbf{1}$, and an identity matrix as \mathbf{I} , with their dimensions either implicitly defined from context or explicitly using subscripts, e.g. $\mathbf{0}_{n_1 \times n_2} \subset \mathbb{R}^{n_1 \times n_2}$, $\mathbf{I}_n \subset \mathbb{R}^{n \times n}$. An empty array is $[\]$. Finally, inequalities \leq, \geq between vectors are compared element-wise.

B. Hybrid Zonotope

A *hybrid zonotope* $\mathcal{HZ}(\mathbf{G}_c, \mathbf{G}_b, \mathbf{c}, \mathbf{A}_c, \mathbf{A}_b, \mathbf{b}) \subset \mathbb{R}^n$ is a set parameterized by a continuous generator matrix $\mathbf{G}_c \in \mathbb{R}^{n \times n_g}$,

a binary generator matrix $\mathbf{G}_b \in \mathbb{R}^{n \times n_b}$, a center $\mathbf{c} \in \mathbb{R}^n$, a continuous linear constraint matrix $\mathbf{A}_c \in \mathbb{R}^{n_c \times n_g}$, a binary linear constraint matrix $\mathbf{A}_b \in \mathbb{R}^{n_c \times n_b}$, and a constraint vector $\mathbf{b} \in \mathbb{R}^{n_c}$ on continuous coefficients $\mathbf{z}_c \in \mathbb{R}^{n_g}$ and binary coefficients $\mathbf{z}_b \in \{-1, 1\}^{n_b}$ as follows [27, Definition 3]:

$$\begin{aligned} & \mathcal{HZ}(\mathbf{G}_c, \mathbf{G}_b, \mathbf{c}, \mathbf{A}_c, \mathbf{A}_b, \mathbf{b}) \\ &= \{ \mathbf{G}_c \mathbf{z}_c + \mathbf{G}_b \mathbf{z}_b + \mathbf{c} \mid \mathbf{A}_c \mathbf{z}_c + \mathbf{A}_b \mathbf{z}_b = \mathbf{b}, \|\mathbf{z}_c\|_\infty \leq 1, \\ & \quad \mathbf{z}_b \in \{-1, 1\}^{n_b} \}. \end{aligned} \quad (1)$$

We denote n_g as the number of continuous generators, n_b as the number of binary generators, and n_c as the number of constraints in a hybrid zonotope.

Consider a pair of hybrid zonotopes $P_1 = \mathcal{HZ}(\mathbf{G}_{c1}, \mathbf{G}_{b1}, \mathbf{c}_1, \mathbf{A}_{c1}, \mathbf{A}_{b1}, \mathbf{b}_1) \subset \mathbb{R}^{n_1}$ and $P_2 = \mathcal{HZ}(\mathbf{G}_{c2}, \mathbf{G}_{b2}, \mathbf{c}_2, \mathbf{A}_{c2}, \mathbf{A}_{b2}, \mathbf{b}_2) \subset \mathbb{R}^{n_2}$. In this paper, we make use of their closed form expressions in generalized intersection under some $\mathbf{R} \subset \mathbb{R}^{n_2 \times n_1}$, denoted as $\cap_{\mathbf{R}}$ [27, Proposition 7]:

$$\begin{aligned} & P_1 \cap_{\mathbf{R}} P_2 = \{ \mathbf{x} \in P_1 \mid \mathbf{R}\mathbf{x} \in P_2 \}, \\ &= \mathcal{HZ} \left(\begin{bmatrix} \mathbf{G}_{c1} & \mathbf{0} \\ \mathbf{G}_{b1} & \mathbf{0} \end{bmatrix}, \begin{bmatrix} \mathbf{c}_1 \\ \mathbf{c}_2 - \mathbf{R}\mathbf{c}_1 \end{bmatrix}, \begin{bmatrix} \mathbf{A}_{c1} & \mathbf{0} \\ \mathbf{0} & \mathbf{A}_{c2} \\ \mathbf{R}\mathbf{G}_{c1} & -\mathbf{G}_{c2} \end{bmatrix}, \right. \\ & \quad \left. \begin{bmatrix} \mathbf{A}_{b1} & \mathbf{0} \\ \mathbf{0} & \mathbf{A}_{b2} \\ \mathbf{R}\mathbf{G}_{b1} & -\mathbf{G}_{b2} \end{bmatrix}, \begin{bmatrix} \mathbf{b}_1 \\ \mathbf{b}_2 \\ \mathbf{c}_2 - \mathbf{R}\mathbf{c}_1 \end{bmatrix} \right). \end{aligned} \quad (2)$$

Note that their ‘‘regular’’ intersection $\{ \mathbf{x} \in P_1 \mid \mathbf{x} \in P_2 \}$, which we denote as $P_1 \cap P_2$, is a particular case of the generalized intersection with $\mathbf{R} = \mathbf{I}$.

Finally, a hybrid zonotope $P = \mathcal{HZ}(\mathbf{G}_c, \mathbf{G}_b, \mathbf{c}, \mathbf{A}_c, \mathbf{A}_b, \mathbf{b}) \subset \mathbb{R}^{n_1}$ is also closed under affine transformation with any matrix $\mathbf{W} \subset \mathbb{R}^{n_2 \times n_1}$ and vector $\mathbf{w} \subset \mathbb{R}^{n_2}$ as [27, Proposition 7]:

$$\begin{aligned} & \mathbf{W}P + \mathbf{w} = \{ \mathbf{W}\mathbf{x} + \mathbf{w} \mid \mathbf{x} \in P \}, \\ &= \mathcal{HZ}(\mathbf{W}\mathbf{G}_c, \mathbf{W}\mathbf{G}_b, \mathbf{W}\mathbf{c} + \mathbf{w}, \mathbf{A}_c, \mathbf{A}_b, \mathbf{b}). \end{aligned} \quad (3)$$

C. ReLU Neural Network

In this work, we consider a fully-connected, ReLU activated feedforward neural network $\xi: \mathbb{R}^{n_0} \rightarrow \mathbb{R}^{n_d}$, with output $\mathbf{x}_d = \xi(\mathbf{x}_0) \in \mathbb{R}^{n_d}$ given an input $\mathbf{x}_0 \in \mathbb{R}^{n_0}$. We denote by $d \in \mathbb{N}$ the *depth* of the network and by n_i the *width* of the i^{th} layer. Mathematically,

$$\mathbf{x}_i = \max(\mathbf{W}_i \mathbf{x}_{i-1} + \mathbf{w}_i, \mathbf{0}), \quad (4a)$$

$$\mathbf{x}_d = \mathbf{W}_d \mathbf{x}_{d-1} + \mathbf{w}_d, \quad (4b)$$

where $\mathbf{W}_i \in \mathbb{R}^{n_i \times n_{i-1}}$, $\mathbf{w}_i \in \mathbb{R}^{n_i}$, $i = 1, \dots, d-1$, $\mathbf{W}_d \in \mathbb{R}^{n_d \times n_{d-1}}$, $\mathbf{w}_d \in \mathbb{R}^{n_d}$, and \max is taken elementwise. We denote $\mathbf{W}_1, \dots, \mathbf{W}_d$ as *weights* and $\mathbf{w}_1, \dots, \mathbf{w}_d$ as *biases* of the network. The function $\max(\cdot, \mathbf{0})$ is known as an n_i -dimensional *ReLU activation function* for $\mathbf{0} \in \mathbb{R}^{n_i}$.

Consider a hybrid zonotope $P_{i-1} \subset \mathbb{R}^{n_{i-1}}$. By applying the operations in (2) and (3), its image through (4a) is exactly a

hybrid zonotope [19], [31]:

$$\begin{aligned} & \{ \max(\mathbf{W}_i \mathbf{x}_{i-1} + \mathbf{w}_i, \mathbf{0}) \mid \mathbf{x}_{i-1} \in P_{i-1} \} \\ &= [\mathbf{0} \quad \mathbf{I}_{n_i}] \left(H_{n_i} \cap [\mathbf{I} \quad \mathbf{0}] (\mathbf{W}_i P_{i-1} + \mathbf{w}_i) \right), \end{aligned} \quad (5)$$

where $H_{n_i} \subset \mathbb{R}^{2n_i}$ is the graph of an n_i -dimensional ReLU activation function over a hypercube domain $\{ \mathbf{x} \mid -a\mathbf{1} \leq \mathbf{x} \leq a\mathbf{1} \}$ for some $a > 0$, which can be represented exactly by a hybrid zonotope as in [31]:

$$\begin{aligned} & H_{n_i} = \left\{ \begin{bmatrix} \mathbf{x} \\ \max(\mathbf{x}, \mathbf{0}) \end{bmatrix} \mid -a\mathbf{1} \leq \mathbf{x} \leq a\mathbf{1} \right\}, \\ &= \mathcal{HZ} \left(\begin{bmatrix} \mathbf{I} \otimes \begin{bmatrix} -\frac{a}{2} & -\frac{a}{2} & 0 & 0 \end{bmatrix} \\ \mathbf{I} \otimes \begin{bmatrix} 0 & -\frac{a}{2} & 0 & 0 \end{bmatrix} \end{bmatrix}, \begin{bmatrix} -\frac{a}{2} \mathbf{I} \\ \mathbf{0} \end{bmatrix}, \frac{a}{2} \mathbf{1}, \right. \\ & \quad \left. \mathbf{I} \otimes [\mathbf{I}_2 \quad \mathbf{I}], \mathbf{I} \otimes \begin{bmatrix} 1 \\ -1 \end{bmatrix}, \mathbf{1} \right), \end{aligned} \quad (6)$$

where \otimes is the Kronecker product. Note that (5) holds as long as a is large enough [19]. As such, the reachable set $P_d \subset \mathbb{R}^{n_d}$ of a hybrid zonotope $Z = P_0 \subset \mathbb{R}^{n_0}$ through a ReLU neural network can be obtained by applying (5) $d-1$ times, before applying an affine transformation parameterized by \mathbf{W}_d and \mathbf{w}_d . This way, if Z has $n_{g,Z}$ continuous generators, $n_{b,Z}$ binary generators, and $n_{c,Z}$ constraints, then P_d will have $n_{g,Z} + n_0 + 4n_n$ continuous generators, $n_{b,Z} + n_n$ binary generators, and $n_{c,Z} + n_0 + 3n_n$ constraints [19], where $n_n := n_1 + \dots + n_{d-1}$ denotes the *number of neurons*.

III. PROBLEM STATEMENT

Our goal in this paper is to design a ReLU neural network training method such that the reachable set of a given input set through the network avoids some unsafe regions. As per most other training methods, we assume that the *structure* (i.e. depth and widths) of the ReLU neural network is fixed as a user choice, and we focus only on updating its weights and biases (a.k.a. trainable parameters). Mathematically, we want to tackle the following problem:

Problem 1 (Training the Reachable Set of a Neural Network to Avoid Unsafe Regions). *Given an input set $Z = \mathcal{HZ}(\mathbf{G}_{c,Z}, \mathbf{G}_{b,Z}, \mathbf{c}_Z, \mathbf{A}_{c,Z}, \mathbf{A}_{b,Z}, \mathbf{b}_Z) \subset \mathbb{R}^{n_0}$ with $n_{g,Z}$ continuous generators, $n_{b,Z}$ binary generators, and $n_{c,Z}$ constraints, an unsafe region $U = \mathcal{HZ}(\mathbf{G}_{c,U}, \mathbf{G}_{b,U}, \mathbf{c}_U, \mathbf{A}_{c,U}, \mathbf{A}_{b,U}, \mathbf{b}_U) \subset \mathbb{R}^{n_d}$ with $n_{g,U}$ continuous generators, $n_{b,U}$ binary generators, and $n_{c,U}$ constraints, and a ReLU neural network ξ with fixed depth d and widths n_0, \dots, n_d , we want to find $\mathbf{W}_1, \dots, \mathbf{W}_d, \mathbf{w}_1, \dots, \mathbf{w}_d$ such that*

$$Q := \{ \xi(\mathbf{x}) \mid \mathbf{x} \in Z \} \cap U = \emptyset. \quad (7)$$

Of course, a trivial solution would be to set $\mathbf{W}_d = \mathbf{0}$ and $\mathbf{w}_d \notin U$, but this kind of solution is not useful. Instead, we aim to design a *differentiable loss function* such that (7) can be achieved by following a gradient and updating the trainable parameters via backpropagation [35]. Doing so allows our method to integrate with other loss functions to achieve additional objectives, as well as makes the training applicable to ReLU networks with other structural constraints, such as when they are embedded in a dynamical system [5]–[7].

IV. METHODS

In this section, we first formulate a MILP to check whether a hybrid zonotope is empty. Then, we explain how to obtain useful gradient information from this MILP to train the ReLU network such that the reachable set is out of the unsafe region.

A. Hybrid Zonotope Emptiness Check

Before constructing a loss function for training, we first need a way to check whether (7) is true. From (2) and (5), the left-hand side of (7), Q , can be straightforwardly computed as a hybrid zonotope $\mathcal{HZ}(\mathbf{G}_{c,Q}, \mathbf{G}_{b,Q}, \mathbf{c}_Q, \mathbf{A}_{c,Q}, \mathbf{A}_{b,Q}, \mathbf{b}_Q) \subset \mathbb{R}^{n_d}$ with $n_{g,Q} = n_{g,Z} + n_0 + 4n_n + n_{g,U}$ continuous generators, $n_{b,Q} = n_{b,Z} + n_n + n_{b,U}$ binary generators, and $n_{c,Q} = n_{c,Z} + n_0 + 3n_n + n_d$ constraints. Then, the image of the input set is not in collision with the unsafe region iff Q is empty. To check whether a hybrid zonotope is empty, existing methods formulate a feasibility MILP with $n_{g,Q}$ continuous variables and $n_{b,Q}$ binary variables [27]:

$$\begin{aligned} & \text{find } \mathbf{z}_c, \mathbf{z}_b, \\ & \text{s.t. } \mathbf{A}_{c,Q}\mathbf{z}_c + \mathbf{A}_{b,Q}\mathbf{z}_b = \mathbf{b}_Q, \\ & \quad \|\mathbf{z}_c\|_\infty \leq 1, \\ & \quad \mathbf{z}_b \in \{-1, 1\}^{n_b}, \end{aligned} \quad (8)$$

which is infeasible iff $Q = \emptyset$. Note that (8) is NP-complete [36]. However, not only is it not always feasible, it is also unclear how to derive a loss function from the optimizers to drive Q to be empty. Instead, consider the following MILP with one more continuous variable than (8):

Proposition 2 (Hybrid Zonotope Emptiness Check). *Given a hybrid zonotope $P = \mathcal{HZ}(\mathbf{G}_c, \mathbf{G}_b, \mathbf{c}, \mathbf{A}_c, \mathbf{A}_b, \mathbf{b}) \subset \mathbb{R}^n$, where $\mathbf{A}_c \in \mathbb{R}^{n_c \times n_g}$ and $\mathbf{A}_b \in \mathbb{R}^{n_c \times n_b}$. Consider the following MILP:*

$$\begin{aligned} & \min r, \\ & \text{s.t. } \mathbf{A}_c\mathbf{z}_c + \mathbf{A}_b\mathbf{z}_b = \mathbf{b}, \\ & \quad \|\mathbf{z}_c\|_\infty \leq r, \\ & \quad \mathbf{z}_b \in \{-1, 1\}^{n_b}, \end{aligned} \quad (9)$$

where $r \in \mathbb{R}$. Then, if r^* is the optimal value of (9), then $P = \emptyset$ iff $r^* > 1$.

Proof. This follows from the definition of hybrid zonotope in (1). \square

By construction, (9) is feasible as long as $\exists \mathbf{z}_c \in \mathbb{R}^{n_g}, \mathbf{z}_b \in \{-1, 1\}^{n_b}$ such that $\mathbf{A}_c\mathbf{z}_c + \mathbf{A}_b\mathbf{z}_b = \mathbf{b}$. If this condition is not met for Q , then we have $Q = \emptyset$ anyway and no training is needed. Importantly, it has been shown in [26] that the minimum upper bound of the norm of the continuous coefficients is useful for gauging the *extent* of collision between two constrained zonotopes, which are subsets of a hybrid zonotope. As such, (9) gives a good foundation for constructing a loss function for encouraging Q to be empty.

B. Loss Function to Encourage Emptiness

We now construct a loss function which, when minimized, makes Q empty. Naively, since $Q = \emptyset$ iff $r^* > 1$, where r^* is the optimal value of (9) with $P = Q$, we can construct the loss function $\ell \in \mathbb{R}$ as:

$$\ell = 1 - r^*, \quad (10)$$

such that when ℓ is decreased to a negative value, we must have $Q = \emptyset$. To minimize ℓ using backpropagation, from chain rule, we must compute $\frac{\partial \ell}{\partial r^*}, \frac{\partial r^*}{\partial \mathbf{A}_{c,Q}}, \frac{\partial r^*}{\partial \mathbf{A}_{b,Q}}, \frac{\partial r^*}{\partial \mathbf{b}_Q}, \frac{\partial r^*}{\partial \mathbf{W}_1}, \dots, \frac{\partial \mathbf{b}_Q}{\partial \mathbf{W}_d}$, and $\frac{\partial \mathbf{A}_{c,Q}}{\partial \mathbf{w}_1}, \dots, \frac{\partial \mathbf{b}_Q}{\partial \mathbf{w}_d}$. Since expressing $\mathbf{A}_{c,Q}, \mathbf{A}_{b,Q}$, and \mathbf{b}_Q in terms of $\mathbf{W}_1, \dots, \mathbf{W}_d$, and $\mathbf{w}_1, \dots, \mathbf{w}_d$ involves only basic matrix operations à la (2) and (5), $\frac{\partial \ell}{\partial r^*}, \frac{\partial \mathbf{A}_{c,Q}}{\partial \mathbf{w}_1}, \dots, \frac{\partial \mathbf{b}_Q}{\partial \mathbf{w}_d}$, and $\frac{\partial \mathbf{A}_{c,Q}}{\partial \mathbf{w}_1}, \dots, \frac{\partial \mathbf{b}_Q}{\partial \mathbf{w}_d}$ can be straightforwardly obtained from automatic differentiation [37]. However, obtaining $\frac{\partial r^*}{\partial \mathbf{A}_{c,Q}}, \frac{\partial r^*}{\partial \mathbf{A}_{b,Q}}$, and $\frac{\partial r^*}{\partial \mathbf{b}_Q}$ involves differentiation through an MILP. Since the optima of an MILP can remain unchanged under small differences in its parameters, its gradient can be 0 or non-existent, which are uninformative [38]. Instead, consider the following convex relaxation of (9):

$$\begin{aligned} & \min \tilde{r} - \mu(\mathbf{1}\ln(\tilde{\mathbf{z}}_{c1}) + \mathbf{1}\ln(\tilde{\mathbf{z}}_{c2}) + \mathbf{1}\ln(\tilde{\mathbf{z}}_b) + \ln(\tilde{r}) + \mathbf{1}\ln(\mathbf{s})), \\ & \text{s.t. } \mathbf{A}_c(\tilde{\mathbf{z}}_{c1} - \tilde{\mathbf{z}}_{c2}) + \mathbf{A}_b(2\tilde{\mathbf{z}}_b - \mathbf{1}) = \mathbf{b}, \\ & \quad \begin{bmatrix} \tilde{\mathbf{z}}_{c1} - \tilde{\mathbf{z}}_{c2} - \tilde{r}\mathbf{1} \\ \tilde{\mathbf{z}}_{c2} - \tilde{\mathbf{z}}_{c1} - \tilde{r}\mathbf{1} \\ \tilde{\mathbf{z}}_b \end{bmatrix} + \mathbf{s} = \begin{bmatrix} \mathbf{0}_{n_c \times 1} \\ \mathbf{0}_{n_c \times 1} \\ \mathbf{1} \end{bmatrix}, \end{aligned} \quad (11)$$

where $\tilde{r} \in \mathbb{R}$, $\tilde{\mathbf{z}}_{c1} \in \mathbb{R}^{n_g}$, $\tilde{\mathbf{z}}_{c2} \in \mathbb{R}^{n_g}$, $\tilde{\mathbf{z}}_b \in \mathbb{R}^{n_b}$, $\mathbf{s} \in \mathbb{R}^{n_g + n_g + n_b}$, $\mu \in \mathbb{R}_+$ is the cut-off multiplier from the solver [39], and $\ln(\cdot)$ is applied elementwise. (11) is the standard linear program (LP) form of (9) with log-barrier regularization and without the integrality constraints, and can be obtained by replacing r with \tilde{r} , \mathbf{z}_c with $\tilde{\mathbf{z}}_{c1} - \tilde{\mathbf{z}}_{c2}$, and \mathbf{z}_b with $2\tilde{\mathbf{z}}_b - \mathbf{1}$ (such that all constraints are non-negative), and introducing slack variable \mathbf{s} (such that inequality constraints become equality constraints) [40].

The optimization problem (11) can be solved quickly using solvers such as IntOpt [39]. Moreover, if \tilde{r}^* is the optimal value of (11), $\frac{\partial \tilde{r}^*}{\partial \mathbf{A}_c}, \frac{\partial \tilde{r}^*}{\partial \mathbf{A}_b}$, and $\frac{\partial \tilde{r}^*}{\partial \mathbf{b}}$ can be obtained by differentiating the Karush-Kuhn-Tucker (KKT) conditions of (11), which we refer the readers to [38, Appendix B] for the mathematical details. Not only are these gradients well-defined, easily computable, and informative, but also, they have been shown to outperform other forms of convex relaxation in computation speed and minimizing loss functions derived from MILPs [38, Appendix E].

Therefore, instead of the loss function ℓ , we propose to backpropagate with respect to a surrogate loss function $\tilde{\ell} \in \mathbb{R}$:

$$\tilde{\ell} = 1 - \tilde{r}^*, \quad (12)$$

where \tilde{r}^* is the optimal value of (11) with $\mathbf{A}_c = \mathbf{A}_{c,Q}$ and $\mathbf{A}_b = \mathbf{A}_{b,Q}$.

Unfortunately, since $\tilde{\ell}$ does not necessarily equal ℓ , we cannot use (12) to simultaneously *verify* and *train* the neural network. In practice, we solve (8) in between some iterations

of training with (12) to check whether (7) has been achieved. If it has, then the training is complete and Problem 1 has been solved.

V. EXPERIMENTS

We now assess the scalability of our method by observing the results under different problem parameters. We also wish to compare our results with [26] to assess our contribution to the state of the art. All experiments were performed on a desktop computer with a 24-core i9 CPU, 32 GB RAM, and an NVIDIA RTX 4090 GPU on Python¹.

A. Experiment Setup and Method

We test our method’s performance under different conditions by varying the width of the first layer $n_1 \in \{10, 20, 30\}$, the depth of the network $d \in \{2, 3, 4\}$, the input dimension $n_0 \in \{2, 4, 6\}$, the output dimension $n_d \in \{2, 4, 6\}$, the complexity of the input set $n_{b,Z} \in \{0, 10, 20\}$, and the complexity of the unsafe region $n_{b,U} \in \{0, 10, 20\}$. We opted not to show results from higher dimensions, set complexities, and larger networks here as we do not wish to introduce large confounding variables from the increased difficulties in training with standard supervised learning.

We define input and unsafe sets as follows. The input set is given by:

$$Z = \mathcal{H}\mathcal{Z} \left\{ \frac{1}{m_Z} \mathbf{I}, \frac{1}{m_Z} \mathbf{1}_{1 \times (m_Z - 1)} \mathbf{I}, \mathbf{0}, [], [], [] \right\}, \quad (13a)$$

$$m_Z = \frac{n_{b,Z}}{n_0} + 1, \quad (13b)$$

which is a hypercube with length 2 centered at the origin formed from a union of $m_Z^{n_0}$ smaller hypercubes (represented as $2^{m_Z - 1}$ overlapping hypercubes). We want its image through the neural network to avoid the unsafe region:

$$U = \mathcal{H}\mathcal{Z} \left\{ \frac{0.5}{m_U} \mathbf{I}, \frac{0.5}{m_U} \mathbf{1}_{1 \times (m_U - 1)} \mathbf{I}, 1.5 \mathbf{1}, [], [], [] \right\}, \quad (14a)$$

$$m_U = \frac{n_{b,U}}{n_d} + 1, \quad (14b)$$

which is a hypercube with length 1 centered at $1.5 \mathbf{1}_{n_d \times 1}$ formed from a union of $m_U^{n_d}$ smaller hypercubes (represented as $2^{m_U - 1}$ overlapping hypercubes). We choose these particular parameters such that the reachable set of the input set and the unsafe region all have shapes similar to those shown in Fig. 2a before we apply our method in IV. Also, when $n_0 = 2$, $n_d = 2$, $n_{b,Z} = 0$, and $n_{b,U} = 0$, we recover the problem setup in [26], which we will compare our method against.

We then ensure our ReLU neural network represents a nonlinear function that intersects the unsafe set. In particular, we use standard supervised learning (implemented in PyTorch [37]) to train the network to approximate a function

$f : \mathbb{R}^{n_0} \rightarrow \mathbb{R}^{n_d}$ defined as:

$$f(\mathbf{x}) = \mathbf{1}_{0.5n_d \times 1} \otimes \begin{bmatrix} x_{\text{odd}}^2 + \sin(x_{\text{even}}) \\ x_{\text{even}}^2 + \sin(x_{\text{odd}}) \end{bmatrix}, \quad (15a)$$

$$x_{\text{odd}} = \frac{1}{\lceil 0.5n_0 \rceil} \sum_{i=1}^{n_0} x_i \mathbb{1}_{\text{odd}}(i), \quad (15b)$$

$$x_{\text{even}} = \frac{1}{\lfloor 0.5n_0 \rfloor} \sum_{i=1}^{n_0} x_i (1 - \mathbb{1}_{\text{odd}}(i)), \quad (15c)$$

where $\lceil \cdot \rceil$ is the ceiling function, $\lfloor \cdot \rfloor$ is the floor function, $\mathbf{x} = [x_1, \dots, x_{n_0}]^T$, and $\mathbb{1}_{\text{odd}} : \mathbb{R}_+ \rightarrow \{0, 1\}$ is the indicator function for odd numbers, such that $\mathbb{1}_{\text{odd}}(i) = 1$ if i is odd and $\mathbb{1}_{\text{odd}}(i) = 0$ if i is even.

Given the pretrained network, we begin training to obey the safety constraint. In each training iteration, we use IntOpt [39] to compute the loss function (12) and PyTorch [37] with `optim.SGD` as the optimizer to update the trainable parameters in the network. Every 10 iterations, we use Gurobi [41] to solve the MILP in (8) to check the emptiness of Q . We are successful in solving Problem 1 if $Q = \emptyset$, at which point we terminate the training instead of updating the parameters. Note that each training iteration is done on CPU instead of GPU. Furthermore, we chose not to solve the MILP in every iteration because solving (8) can be many times slower than solving (11).

We also compare against a constrained zonotope safe training method [26]. We tested the method with $n_1 = 10$, $d = 2$, $n_0 = 2$, $n_d = 2$, $n_{b,Z} = 0$, and $n_{b,U} = 0$, which are the parameters used in the example in [26]. To compare the scalability of both methods, we also tested [26] on $n_1 = 20$ and $n_1 = 30$. To ensure fairness, we do not include the objective loss and only add the constraint loss when it is positive (see [26] for details). We terminate the training once the constraint loss has reached zero (i.e. the reachable set is out of collision with the unsafe set).

B. Hypotheses

Since the most complex operations in our method are solving the relaxed LP (11) and the MILP (8), we expect our performance to be dependent on the solvers’ (i.e. IntOpt and Gurobi) ability to scale with the number of variables and constraints, which in turn scale linearly with the dimensions, network size, and set complexity (see Sec. IV-A). As such, we expect the computation time for each iteration of our method to be significantly faster than that of [26], which scales *exponentially* with the number of neurons. That said, since [26] verifies (7) in every iteration (whereas our method only checks it every 10 iterations), it is also possible for [26] to terminate the training earlier than our method does.

C. Results and Discussion

We report the results of our experiments in Table I. All reachable sets have been successfully driven out of the unsafe regions, except for [26] with n_1 of 30, which failed to even compute the reachable set. We show the training progression of one of the experiments in Fig. 2, which clearly shows the loss function driving the reachable set out of collision.

¹We are preparing our code for open-source release

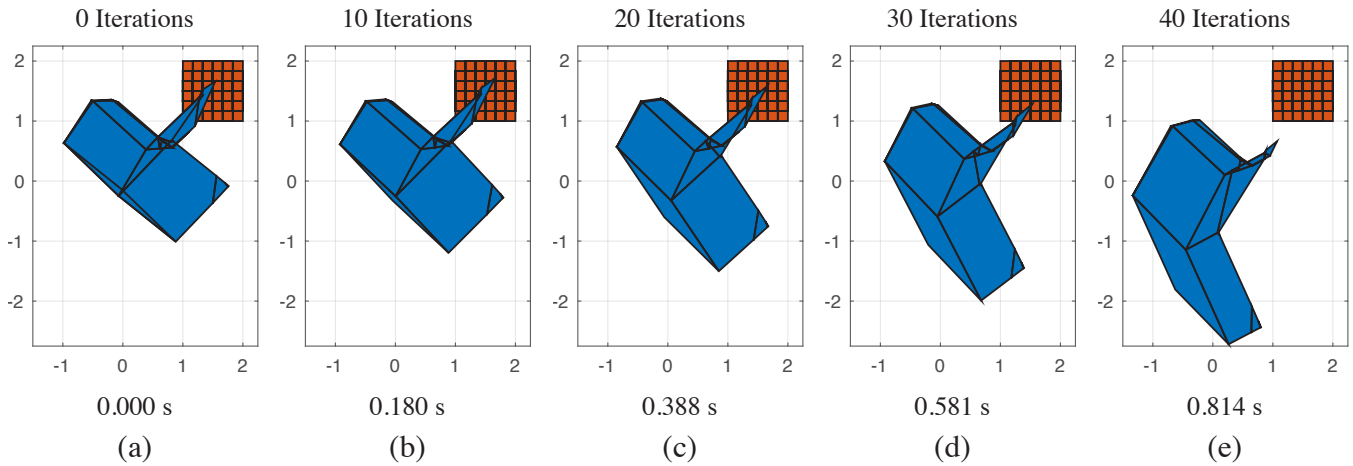


Fig. 2. Training an input set's reachable set (blue) through a neural network to avoid the unsafe region (red) after (a) 0, (b) 10, (c) 20, (d) 30, and (e) 40 iterations with our method, with network size (2, 10, 2), $n_{b,Z} = 0$, and $n_{b,Q} = 10$. The elapsed times are denoted below the figures. Our algorithm treats the unsafe region as a union of 2^{10} overlapping convex sets.

As expected, the computation time of our method is largely dictated by the complexity of the LP and MILP problem. In theory, since IntOpt [39] is a primal-dual interior point solver, it has a complexity of $\mathcal{O}(k\sqrt{n_{g,Q} + n_{b,Q}})$ [42], where k is the bit length of the input data. On the other hand, since (8) is NP-complete, it has a worst-case complexity of $\mathcal{O}(2^{n_{b,Q}})$ [36]. In the experiments in this section, solving (8) was on average 2 to 4 times longer than solving (11). To circumvent this for more complex problems, we can either lower the frequency of calling (8) (i.e. increase the number of iterations between calling the MILP), or replace (8) with faster but over-approximative neural network verification methods such as [21]. In other words, our method can *modular* to other neural network verification techniques.

We believe the power of our method comes from the low complexity of hybrid zonotope representation (specifically, Q), which scales only linearly with the number of neurons, input and output dimensions, and complexity of the input set and the unsafe region. For example, when increasing $n_{b,Z}$ from 10 to 20, the maximum number of convex sets representable as a union by Z increases from 2^{10} to 2^{20} , even though only 10 more binary (continuous in the LP's case) variables are needed, adding only 0.056 s of computation time to every 10 iterations. In contrast, since the complexity of the constrained zonotope representation in [26] increases exponentially with the number of neurons in the method, our method easily outperforms it for larger network sizes. For a more detailed discussion on the scalability and representation power of hybrid zonotopes, we refer the reader to [19] and [27].

VI. DEMONSTRATION

We now demonstrate our method's ability to handle deep neural networks and disjoint, non-convex input and unsafe sets. To the best of our knowledge, no existing method can solve this problem with formal guarantees.

A. Demonstration Setup

In this experiment, we first train a ReLU neural network with $d = 4$ and $n_1 = n_2 = n_3 = 30$ to approximate (15), where $n_0 = n_d = 2$. We choose the input set as the union of 7 V-polytopes (i.e. polytopes represented by vertices) $Z = \bigcup_{i=1}^7 Z_i$, where

$$\begin{aligned} Z_1 &= \text{conv}([0, 1]^T, [0.2, 0.2]^T, [-0.2, 0.2]^T), \\ Z_2 &= \text{conv}([-0.2, 0.2]^T, [-0.2, -0.2]^T, [-1, 0]^T), \\ Z_3 &= \text{conv}([0.2, -0.2]^T, [0, -0.1]^T, [-0.2, -0.2]^T), \\ Z_4 &= \text{conv}([0.2, 0.2]^T, [1, 0]^T, [0.2, -0.2]^T), \\ Z_5 &= \text{conv}([-1, 1]^T, [-0.1, 1]^T, [-0.28, 0.28]^T, [-1, 0.1]^T), \\ Z_6 &= \text{conv}([0.1, 1]^T, [1, 1]^T, [1, 0.1]^T), \text{ and} \\ Z_7 &= \text{conv}([1, -0.1]^T, [1, -1]^T, [0.1, -1]^T, [0.28, -0.28]^T), \end{aligned}$$

where $\text{conv}(\cdot)$ is the convex hull operation. Similarly, we choose the unsafe set as the union of 3 V-polytopes $U = \bigcup_{i=1}^3 U_i$, where

$$\begin{aligned} U_1 &= \text{conv}([1, 2]^T, [2, 2]^T, [2, 1]^T), \\ U_2 &= \text{conv}([1.5, 0]^T, [2, -0.5]^T, [1.5, -1]^T), \text{ and} \\ U_3 &= \text{conv}([-0.5, 2]^T, [0, 1.5]^T, [-1, 1.5]^T). \end{aligned}$$

See Fig. 1 for a visualization of the sets. Note that a union of n_N V-polytopes with a total of n_v vertices can be *exactly* represented as a hybrid zonotope with $2n_v$ continuous generators, n_N binary generators, and $n_v + 2$ constraints [43], and can be further simplified using reduction algorithms [34].

We use the same solvers and computer with Sec. V. As before, we verify the satisfaction of (7) every 10 iterations using (8).

B. Results and Discussion

The results of the experiment are shown in Table I and visualized in Fig. 1. Since the complexity of the set representations and the network size are significantly larger than those in Sec. V, the number of constraints and variables

TABLE I

Summary of duration required to drive a neural network’s reachable set (i.e. image of a given input set) out of an unsafe region under different network sizes, input and output dimensions, and complexity of the input set and the unsafe region. The dimensions of the hybrid zonotope intersection of the reachable set and the unsafe region $n_{g,Q}$, $n_{c,Q}$, and $n_{b,Q}$ represents the complexity of the LPs and MILPs that must be solved during the training iterations, which took up a majority of the computation time.

Method	Network Size (n_0, \dots, n_d)	$n_{b,Z}$	$n_{b,U}$	Time (s)	Iterations	Time per 10 Iterations (s)	$n_{c,Q}$	$n_{g,Q}$	$n_{b,Q}$
Sec. V									
Increasing Network Width Increases Training Time in Each Iteration									
Ours	(2, 10, 2)	0	0	1.318	70	0.188	32	44	10
	(2, 20, 2)	0	0	12.960	130	0.997	62	84	20
	(2, 30, 2)	0	0	17.721	60	2.954	92	124	30
[26] Scales Very Poorly with Increasing Network Width									
[26]	(2, 10, 2)	0	0	0.755	2	3.775	N/A	N/A	N/A
	(2, 20, 2)	0	0	946.677	3	3,155.590	N/A	N/A	N/A
	(2, 30, 2)	0	0	Timeout	N/A	Timeout	N/A	N/A	N/A
Increasing Network Depth Increases Training Time in Each Iteration									
Ours	(2, 10, 10, 2)	0	0	0.879	10	0.879	62	84	20
	(2, 10, 10, 10, 2)	0	0	5.709	20	2.855	92	124	30
Increasing Input Dimension Increases Training Time in Each Iteration									
Ours	(4, 10, 2)	0	0	0.167	10	0.167	32	46	10
	(6, 10, 2)	0	0	0.450	20	0.225	32	48	10
Increasing Output Dimension Increases Training Time in Each Iteration									
Ours	(2, 10, 4)	0	0	5.756	270	0.195	34	46	10
	(2, 10, 6)	0	0	0.191	10	0.191	36	48	10
Increasing Input Set Complexity Increases Training Time in Each Iteration									
Ours	(2, 10, 2)	10	0	0.859	40	0.215	32	44	20
	(2, 10, 2)	20	0	2.165	80	0.271	32	44	30
Increasing Unsafe Set Complexity Increases Training Time in Each Iteration									
Ours	(2, 10, 2)	0	10	0.814	40	0.204	32	44	20
	(2, 10, 2)	0	20	2.451	90	0.272	32	44	30
Sec. VI									
Ours	(2, 30, 30, 30, 2)	7	3	490.290	20	245.145	309	426	100

in the LPs and MILPs solved are also a magnitude larger. Despite this, our method is still able to drive the reachable set out of collision with the unsafe set in 20 iterations after 490.290 s. A majority of the computation time was spent solving the MILPs, which took 54.740 s and 194.987 s at the 10th and 20th iteration. In contrast, solving (11) took less than 0.1 s in each iteration.

This demo presents preliminary results on how to train a neural network to obey non-convex constraints with formal guarantees *for the first time*. However, it also reveals the method’s computational bottleneck of solving the NP-complete problem in (8), which limits its utility in applications that require larger networks and more complex sets. We plan to address this in future work by experimenting with other neural network verification techniques, or by developing over-approximation methods using hybrid zonotopes with simpler representations.

VII. CONCLUSION

This work proposes a new training method for enforcing constraint satisfaction by extracting learning signals from neural network reachability analysis using hybrid zonotopes. This method is exact and can handle non-convex input sets and unsafe regions, and has been shown to be fast and scale fairly well with respect to network sizes, dimensions, and set complexities, significantly outperforming our previous work in [26].

Limitations: Our current implementation has several drawbacks to be addressed in future work. Firstly, while the training step remains fast and efficient with an increase in network sizes and set complexities, the verification step does not, since the MILP in (8) is NP-complete. Secondly, the method is limited to fully-connected networks with ReLU activation functions, which prevents it from being applied to more interesting problems such as those with convolutional

neural networks (CNNs) or those with neural networks embedded in dynamical systems. Finally, as with other neural network training methods, backpropagation through the loss function does not guarantee convergence towards the global minimum. Thus, our method cannot guarantee the discovery of a solution, even if it exists.

Future Work: Going forward, we hope to explore our method’s compatibility with other verification methods to overcome the NP-complete problem in solving the MILP, at the cost of potentially losing exactness. We also plan to apply techniques from [31], [33], [34] to train ReLU networks embedded in dynamical systems, and leverage tricks from [18] to apply hybrid zonotope techniques on CNNs. If successful, they could advance safety in camera-based control for autonomous driving [16] or aircraft landing [44]–[46].

Another particularly exciting possibility this method can enable is a form of *set-based training*, where instead of training a neural network with features and labels as *points*, we can represent them as *sets* around the points, which can make the network provably robust against attacks and disturbances for seen examples. This could be enabled by solving the optimization problems (8) and (11) in parallel on GPU using methods similar to [47].

REFERENCES

- [1] M. Leshno, V. Y. Lin, A. Pinkus, and S. Schocken, “Multilayer feedforward networks with a nonpolynomial activation function can approximate any function,” *Neural networks*, vol. 6, no. 6, pp. 861–867, 1993.
- [2] G. Dulac-Arnold, N. Levine, D. J. Mankowitz, *et al.*, “Challenges of real-world reinforcement learning: definitions, benchmarks and analysis,” *Machine Learning*, vol. 110, no. 9, pp. 2419–2468, 2021.
- [3] K. Eykholt, I. Evtimov, E. Fernandes, *et al.*, “Robust physical-world attacks on deep learning visual classification,” in *Proceedings of the IEEE conference on computer vision and pattern recognition*, 2018, pp. 1625–1634.
- [4] C. Szegedy, “Intriguing properties of neural networks,” *arXiv preprint arXiv:1312.6199*, 2013.
- [5] B. Ko, H.-J. Choi, C. Hong, J.-H. Kim, O. C. Kwon, and C. D. Yoo, “Neural network-based autonomous navigation for a homecare mobile robot,” in *2017 IEEE International Conference on Big Data and Smart Computing (BigComp)*, IEEE, 2017, pp. 403–406.
- [6] E. N. Johnson, A. J. Calise, and J. E. Corban, “Adaptive guidance and control for autonomous launch vehicles,” in *2001 IEEE Aerospace Conference Proceedings (Cat. No. 01TH8542)*, IEEE, vol. 6, 2001, pp. 2669–2682.
- [7] J. Ni, Y. Chen, Y. Chen, J. Zhu, D. Ali, and W. Cao, “A survey on theories and applications for self-driving cars based on deep learning methods,” *Applied Sciences*, vol. 10, no. 8, p. 2749, 2020.
- [8] N. H. T. S. Administration *et al.*, “Summary report: standing general order on crash reporting for level 2 advanced driver assistance systems,” *US Department of Transport*, 2022.
- [9] L. Brunke, M. Greeff, A. W. Hall, *et al.*, “Safe learning in robotics: From learning-based control to safe reinforcement learning,” *Annual Review of Control, Robotics, and Autonomous Systems*, vol. 5, no. 1, pp. 411–444, 2022.
- [10] S. Gu, L. Yang, Y. Du, *et al.*, “A review of safe reinforcement learning: Methods, theory and applications,” *arXiv preprint arXiv:2205.10330*, 2022.
- [11] Z. Liu, Z. Guo, Y. Yao, *et al.*, “Constrained decision transformer for offline safe reinforcement learning,” in *International Conference on Machine Learning*, PMLR, 2023, pp. 21 611–21 630.
- [12] K. Chakraborty, A. Gupta, and S. Bansal, “Enhancing Safety and Robustness of Vision-Based Controllers via Reachability Analysis,” *arXiv preprint arXiv:2410.21736*, 2024.
- [13] K.-C. Hsu, D. P. Nguyen, and J. F. Fisac, “Isaacs: Iterative soft adversarial actor-critic for safety,” in *Learning for Dynamics and Control Conference*, PMLR, 2023, pp. 90–103.
- [14] R. Balestriero and Y. LeCun, “POLICE: Provably optimal linear constraint enforcement for deep neural networks,” in *ICASSP 2023-2023 IEEE International Conference on Acoustics, Speech and Signal Processing (ICASSP)*, IEEE, 2023, pp. 1–5.
- [15] J.-B. Bouvier, K. Nagpal, and N. Mehr, “POLICEd RL: Learning Closed-Loop Robot Control Policies with Provable Satisfaction of Hard Constraints,” *arXiv preprint arXiv:2403.13297*, 2024.
- [16] H.-D. Tran, X. Yang, D. Manzananas Lopez, *et al.*, “NNV: the neural network verification tool for deep neural networks and learning-enabled cyber-physical systems,” in *International Conference on Computer Aided Verification*, Springer, 2020, pp. 3–17.
- [17] H.-D. Tran, D. Manzananas Lopez, P. Musau, *et al.*, “Star-based reachability analysis of deep neural networks,” in *Formal Methods—The Next 30 Years: Third World Congress, FM 2019, Porto, Portugal, October 7–11, 2019, Proceedings 3*, Springer, 2019, pp. 670–686.
- [18] H.-D. Tran, S. Bak, W. Xiang, and T. T. Johnson, “Verification of deep convolutional neural networks using imagestars,” in *International conference on computer aided verification*, Springer, 2020, pp. 18–42.
- [19] J. Ortiz, A. Vellucci, J. Koeln, and J. Ruths, “Hybrid zonotopes exactly represent ReLU neural networks,” in *2023 62nd IEEE Conference on Decision and Control (CDC)*, IEEE, 2023, pp. 5351–5357.
- [20] Y. Zhang and X. Xu, “Safety verification of neural feedback systems based on constrained zonotopes,” in *2022 IEEE 61st Conference on Decision and Control (CDC)*, IEEE, 2022, pp. 2737–2744.
- [21] H. Zhang, T.-W. Weng, P.-Y. Chen, C.-J. Hsieh, and L. Daniel, “Efficient neural network robustness certification with general activation functions,” *Advances in neural information processing systems*, vol. 31, 2018.
- [22] N. Kochdumper, C. Schilling, M. Althoff, and S. Bak, “Open- and closed-loop neural network verification using polynomial zonotopes,” in *NASA Formal Methods Symposium*, Springer, 2023, pp. 16–36.
- [23] T. Ladner and M. Althoff, “Automatic abstraction refinement in neural network verification using sensitivity analysis,” in *Proceedings of the 26th ACM International Conference on Hybrid Systems: Computation and Control*, 2023, pp. 1–13.
- [24] A. Harapanahalli and S. Coogan, “Certified Robust Invariant Polytope Training in Neural Controlled ODEs,” *arXiv preprint arXiv:2408.01273*, 2024.
- [25] J. K. Scott, D. M. Raimondo, G. R. Marseglia, and R. D. Braatz, “Constrained zonotopes: A new tool for set-based estimation and fault detection,” *Automatica*, vol. 69, pp. 126–136, 2016.
- [26] L. K. Chung, A. Dai, D. Knowles, S. Kousik, and G. X. Gao, “Constrained feedforward neural network training via reachability analysis,” *arXiv preprint arXiv:2107.07696*, 2021.
- [27] T. J. Bird, H. C. Pangborn, N. Jain, and J. P. Koeln, “Hybrid zonotopes: A new set representation for reachability analysis of mixed logical dynamical systems,” *Automatica*, vol. 154, p. 111 107, 2023.
- [28] T. J. Bird and N. Jain, “Unions and complements of hybrid zonotopes,” *IEEE Control Systems Letters*, vol. 6, pp. 1778–1783, 2021.
- [29] J. Koeln, T. J. Bird, J. Siefert, J. Ruths, H. C. Pangborn, and N. Jain, “zonoLAB: A MATLAB toolbox for set-based control systems analysis using hybrid zonotopes,” in *2024 American Control Conference (ACC)*, IEEE, 2024, pp. 2513–2520.
- [30] L. Hadjiloizou, F. J. Jiang, A. Alanwar, and K. H. Johansson, “Formal Verification of Linear Temporal Logic Specifications Using Hybrid Zonotope-Based Reachability Analysis,” *arXiv preprint arXiv:2404.03308*, 2024.
- [31] Y. Zhang, H. Zhang, and X. Xu, “Backward reachability analysis of neural feedback systems using hybrid zonotopes,” *IEEE Control Systems Letters*, vol. 7, pp. 2779–2784, 2023.
- [32] T. J. Bird, J. A. Siefert, H. C. Pangborn, and N. Jain, “A set-based approach for robust control co-design,” in *2024 American Control Conference (ACC)*, IEEE, 2024, pp. 2564–2571.
- [33] H. Zhang, Y. Zhang, and X. Xu, “Hybrid Zonotope-Based Backward Reachability Analysis for Neural Feedback Systems With Nonlinear Plant Models,” in *2024 American Control Conference (ACC)*, IEEE, 2024, pp. 4155–4161.

- [34] Y. Zhang and X. Xu, "Reachability analysis and safety verification of neural feedback systems via hybrid zonotopes," in *2023 American Control Conference (ACC)*, IEEE, 2023, pp. 1915–1921.
- [35] D. E. Rumelhart, G. E. Hinton, and R. J. Williams, "Learning representations by back-propagating errors," *nature*, vol. 323, no. 6088, pp. 533–536, 1986.
- [36] T. Achterberg, R. E. Bixby, Z. Gu, E. Rothberg, and D. Weninger, "Presolve reductions in mixed integer programming," *INFORMS Journal on Computing*, vol. 32, no. 2, pp. 473–506, 2020.
- [37] A. Paszke, S. Gross, F. Massa, *et al.*, "Pytorch: An imperative style, high-performance deep learning library," *Advances in neural information processing systems*, vol. 32, 2019.
- [38] X. Hu, J. Lee, and J. Lee, "Two-Stage Predict+ Optimize for MILPs with Unknown Parameters in Constraints," *Advances in Neural Information Processing Systems*, vol. 36, 2024.
- [39] J. Mandi and T. Guns, "Interior point solving for lp-based prediction+ optimisation," *Advances in Neural Information Processing Systems*, vol. 33, pp. 7272–7282, 2020.
- [40] S. Boyd and L. Vandenberghe, *Convex optimization*. Cambridge university press, 2004.
- [41] L. Gurobi Optimization, *Gurobi optimizer reference manual*, 2021.
- [42] S. J. Wright, *Primal-dual interior-point methods*. SIAM, 1997.
- [43] J. A. Siefert, T. J. Bird, A. F. Thompson, *et al.*, "Reachability analysis using hybrid zonotopes and functional decomposition," *IEEE Transactions on Automatic Control*, 2025.
- [44] M. J. Kochenderfer and J. Chryssanthacopoulos, "Robust airborne collision avoidance through dynamic programming," *Massachusetts Institute of Technology, Lincoln Laboratory, Project Report ATC-371*, vol. 130, 2011.
- [45] M. J. Kochenderfer, J. E. Holland, and J. P. Chryssanthacopoulos, "Next generation airborne collision avoidance system," *Lincoln Laboratory Journal*, vol. 19, no. 1, pp. 17–33, 2012.
- [46] M. J. Kochenderfer, C. Amato, G. Chowdhary, *et al.*, "Optimized airborne collision avoidance," 2015.
- [47] B. Amos and J. Z. Kolter, "Optnet: Differentiable optimization as a layer in neural networks," in *International conference on machine learning*, PMLR, 2017, pp. 136–145.